

Shifted-elementary-mode representation for partially coherent vectorial fields

Jani Tervo, Jari Turunen, and Pasi Vahimaa

University of Eastern Finland, Department of Physics and Mathematics, P.O. Box 111, FI-80101 Joensuu, Finland

Frank Wyrowski

Friedrich Schiller University of Jena, Department of Applied Physics, D-07745 Jena, Germany

A representation of partially spatially coherent and partially polarized stationary electromagnetic fields is given in terms of mutually uncorrelated, transversely shifted, fully coherent and polarized elementary electric-field modes. This representation allows one to propagate non-paraxial partially coherent vector fields using techniques for spatially fully coherent fields, which are numerically far more efficient than methods for propagating correlation functions. A procedure is given to determine the elementary modes from the radiant intensity and the far-zone polarization properties of the entire field. The method is applied to quasihomogeneous fields with rotationally symmetric $\cos^n \theta$ radiant intensity distributions (θ being the diffraction angle with respect to the optical axis and n an integer). This is an adequate model for fields emitted by, e.g., many light-emitting diodes.

© 2010 Optical Society of America

OCIS codes: 030.1640, 260.5430, 050.1940,

1. Introduction

There is a growing demand to include partial spatial coherence in optical design, not only because of classical areas of application such as microscopy and projection lithography, but also because of the increasing importance of partially coherent solid-state sources such as multimode lasers (including excimers) and LEDs. Methods based on ray optics can not adequately describe all of the relevant issues related to coherence and polarization, which are intimately connected in electromagnetic coherence theory. Thus wave-optical methods are required, which must be capable of dealing with non-paraxial fields and systems that may contain also micro- and nanostructures in objects and interfaces. To this end, one needs computationally efficient physical-optics-based representations of spatially partially coherent electromagnetic fields.

Apart from some specific models that allow analytic solutions, propagating spatially partially coherent light even in free space is a formidable numerical problem involving four-dimensional integrals [1]. The dimensionality of the propagation integrals can be decreased to two (for planar sources) if the partially coherent field is represented as an incoherent superposition of fully spatially coherent fields. The classical way to do this is the coherent-mode expansion of the cross-spectral density (CSD) function by means of Mercer's expansion [2], which has recently been extended to electromagnetic fields [3, 4]. In this representation the coherent modes are uniquely defined by the CSD through a Fredholm integral equation; they form a complete and orthonormal set, in which the effective number of modes N increases as the degree of coherence of the field is reduced [5–8]. Thus, in free-

space propagation, the original four-dimensional integral for CSD is replaced by N two-dimensional integrals for the coherent modes. In light-matter interaction analysis one solves the diffraction or scattering problem for N coherent fields of different functional forms [9, 10].

There is also an alternative representation of a partially coherent field in terms of uncorrelated, fully coherent fields [11–15]. Here all coherent fields or 'elementary modes' are of identical functional form but spatially (or angularly) shifted with respect to each other and weighted by a function determined by the CSD. Unlike the Mercer expansion, the shifted-elementary-mode representation is applicable only to a specific class of genuine CSDs [14]. However, this class contains many of the fields of practical significance in optical design, including all quasihomogeneous fields (LEDs, excimers, illumination in microscopy and projection lithography, etc.). Since the elementary modes are identical, only a single 2D integral needs to be evaluated in free-space propagation problems. In interaction problems one needs to scan the elementary mode across the object and perform a set of independent diffraction calculations for coherent light. Typically the elementary mode has a smooth functional form, at least compared to the higher-order modes in the Mercer expansion, and is therefore easy to propagate numerically. Another advantage of the shifted-mode model is that there is no need for numerical solution of the Fredholm integral equation: the elementary mode and the associated weight function can be determined, e.g., from far-zone properties of the field [13].

In this paper we generalize the scalar shifted-elementary-mode representation to the vectorial case, which is necessary to adequately model partially spatially coherent, partially polarized sources. There are two ma-

for reasons why such a generalization is necessary: first, non-paraxial fields can not be adequately described by a scalar model and, second, optical components in the system can modify the polarization state of the field. It turns out that the vectorial nature of the field does not fundamentally complicate the numerical procedure. Two elementary modes are needed to specify the state of polarization, but also in the electromagnetic case the modes and their weight functions can be determined from far-zone properties of the field.

We begin the discussion by briefly reviewing the scalar model in Sect. 2 to establish the notation and to simplify the interpretation of the main results. The extension to the electromagnetic case is outlined in Sect. 3 and the rigorous mathematical formulation is presented Sections 4 and 5. The important special case of rotationally symmetric and quasihomogeneous fields is discussed in Sections 6 and 7, respectively. Some numerical results are provided in Sect. 8. In Sect. 9 we apply the model to a simple LED geometry. Finally, issues such as the measurements required to determine the elementary modes and their weight functions are discussed in Sect. 10.

2. The scalar model

Using the notations of Fig. 1, we may write the well-known relationship [1] between the cross-spectral density function $W(\mathbf{r}_1, \mathbf{r}_2)$ and the angular correlation function $A(\boldsymbol{\kappa}_1, \boldsymbol{\kappa}_2)$ as (we omit the dependence on the angular frequency ω for brevity throughout the paper)

$$W(\mathbf{r}_1, \mathbf{r}_2) = \frac{1}{(2\pi)^4} \iiint \iiint_{-\infty}^{\infty} A(\boldsymbol{\kappa}_1, \boldsymbol{\kappa}_2) \times \exp[i(\mathbf{k}_2 \cdot \mathbf{r}_2 - \mathbf{k}_1^* \cdot \mathbf{r}_1)] d^2\kappa_1 d^2\kappa_2. \quad (1)$$

Here the asterisk indicates complex conjugation, $\mathbf{r}_j = (x_j, y_j, z_j)$ with $j = 1, 2$ are position vectors, $\mathbf{k}_j = (k_{jx}, k_{jy}, k_{jz}) = (\boldsymbol{\kappa}_j, k_{jz})$ represent wave vectors, and $\boldsymbol{\kappa}_j = (k_{jx}, k_{jy})$ are their transverse projections.

Restricting now to the specific class of fields mentioned in the introduction, we assume that the angular correlation function is of the Schell-model form [13]

$$A(\boldsymbol{\kappa}_1, \boldsymbol{\kappa}_2) = g(\Delta\boldsymbol{\kappa}) f^*(\boldsymbol{\kappa}_1) f(\boldsymbol{\kappa}_2). \quad (2)$$

The radiant intensity of a scalar field is defined as [1]

$$J(r\hat{\mathbf{s}}) = 2n\pi^2 k^2 \cos^2 \theta A(k\boldsymbol{\sigma}, k\boldsymbol{\sigma}), \quad (3)$$

where n is the refractive index of the medium, $\hat{\mathbf{s}} = \mathbf{r}/r$ with $r = \|\mathbf{r}\|$ is a unit direction vector, $\boldsymbol{\sigma}$ is its transverse projection, θ is the angle between $\hat{\mathbf{s}}$ and the z axis, and $k = \|\mathbf{k}\|$ is the wave number. Using Eq. (2), we have

$$J(r\hat{\mathbf{s}}) = 2n\pi^2 k^2 \cos^2 \theta |f(k\boldsymbol{\sigma})|^2 \quad (4)$$

Thus the radiant intensity of a Schell-model partially coherent field defined by Eq. (2) is the same as that produced by a coherent field with angular spectrum $f(\boldsymbol{\kappa})$.

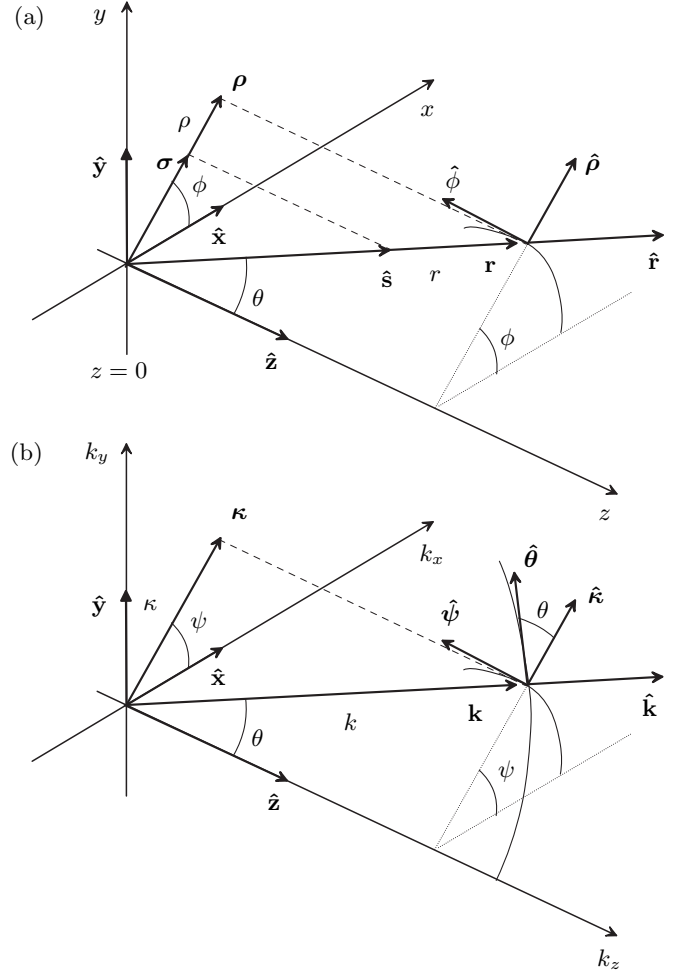


Fig. 1. Notations used for (a) position and (b) wave-vector coordinates.

Let us introduce two-dimensional Fourier-transform relations

$$e(\mathbf{r}) = \frac{1}{(2\pi)^2} \iint_{-\infty}^{\infty} f(\boldsymbol{\kappa}) \exp(i\mathbf{k} \cdot \mathbf{r}) d^2\kappa \quad (5)$$

and

$$p(\boldsymbol{\rho}) = \frac{1}{(2\pi)^2} \iint_{-\infty}^{\infty} g(\Delta\boldsymbol{\kappa}) \exp(i\Delta\boldsymbol{\kappa} \cdot \boldsymbol{\rho}) d^2\Delta\kappa, \quad (6)$$

where $\Delta\boldsymbol{\kappa} = \boldsymbol{\kappa}_2 - \boldsymbol{\kappa}_1$ and $\boldsymbol{\rho} = x\hat{\mathbf{x}} + y\hat{\mathbf{y}}$ is the transverse projection of the position vector. Inserting Eq. (2) into Eq. (1) and using the Fourier representation of $g(\Delta\boldsymbol{\kappa})$ obtained by inverting Eq. (6), we get the expression

$$W(\mathbf{r}_1, \mathbf{r}_2) = \iint_{-\infty}^{\infty} p(\boldsymbol{\rho}') e^*(\mathbf{r}_1 - \boldsymbol{\rho}') e(\mathbf{r}_2 - \boldsymbol{\rho}') d^2\rho' \quad (7)$$

for the CSD [13]. This result applies, in particular, at $z = 0$. Thus $e(\boldsymbol{\rho}, 0)$ is the coherent source-plane field with

angular spectrum $f(\boldsymbol{\kappa})$. The representation in Eq. (7) expresses the partially coherent field as a weighted linear superposition of spatially shifted but identical fully coherent elementary (scalar) fields $e(\boldsymbol{\rho}, 0)$.

3. The electromagnetic extension

As is evident from Eq. (3), the mathematical form of the elementary field mode $e(\boldsymbol{\rho}, 0)$ can be determined from the knowledge of the radiant intensity (at least apart from a phase factor, which can in fact be employed to model volume sources [15]). In general, the weight function $p(\boldsymbol{\rho}')$ can be determined from far-field coherence measurements using Eqs. (2) and (6), but often there are simpler ways to at least approximate it [13]. This is the case, in particular, if the field is quasihomogeneous, i.e., if the coherence area in the source plane is much smaller than source area; in this case the weight function comes out of the integral in Eq. (7). When $e(\boldsymbol{\rho}, 0)$ and $p(\boldsymbol{\rho}')$ are known, coherent propagation techniques for $e(\boldsymbol{\rho}, 0)$ and a linear superposition according to Eq. (7) suffice to propagate the entire spatially partially coherent field.

The extension of the scalar shifted-mode model to the electromagnetic case is not trivial. One might be tempted to use some superpositions of, e.g., locally linearly polarized modes of the scalar functional form to model partially polarized or unpolarized sources. However, such constructions seem hard to justify mathematically. The approach taken here is based on far-field information: in the far zone the field behaves as an outgoing spherical wave, and therefore it has a well-defined local polarization state. We employ this fact to separate the angular correlation tensor, which is the electromagnetic extension of the function $A(\boldsymbol{\kappa}_1, \boldsymbol{\kappa}_2)$, into two orthogonal parts [see Eq. (30) in sect. 4]. These represent the electromagnetic elementary modes (or polarization modes) in the far field. Then the source-plane modes can be determined by Fourier-transform techniques in analogy with the scalar case.

As a result of the construction process (to be described mathematically in the following sections), we obtain a vectorial shifted-mode expansion for the spatially partially coherent field everywhere in space [see Eqs. (32), (33), and (40) in Sect. 5]. Instead of propagating one fully coherent mode as in the scalar case, we now need to propagate two well-defined fully coherent vectorial field modes, and to form the generalized shifted-mode superposition, to govern the propagation of the electromagnetic spatially partially coherent field. Thus the increase in computational complexity, compared to the scalar case, is essentially fourfold.

4. Field representation in the far-zone

A statistically stationary random electromagnetic field in the space-frequency domain is described by a CSD matrix $\mathcal{W}(\mathbf{r}_1, \mathbf{r}_2)$, which may be expressed as [4, 16]

$$\mathcal{W}(\mathbf{r}_1, \mathbf{r}_2) = \langle \mathbf{E}^*(\mathbf{r}_1) \mathbf{E}^T(\mathbf{r}_2) \rangle. \quad (8)$$

Here T indicates the transpose, the brackets denote ensemble averaging, and the electric-field realizations $\mathbf{E}(\mathbf{r})$ are understood as appropriate random linear superpositions of the eigenfunctions of the Fredholm integral equation satisfied by $\mathcal{W}(\mathbf{r}_1, \mathbf{r}_2)$ [3, 4]. The position-dependent spectral density of the field can be written, in analogy with scalar theory of partial coherence [2], as $S(\mathbf{r}) = \text{tr } \mathcal{W}(\mathbf{r}, \mathbf{r})$, where tr stands for trace.

The relation between the field at the (secondary) source plane $z = 0$ and the far-field can be found, for example, using the angular spectrum representation of the CSD matrix [17]. We thus have, at any plane $z > 0$,

$$\begin{aligned} \mathcal{W}(\mathbf{r}_1, \mathbf{r}_2) &= \frac{1}{(2\pi)^4} \iiint \int_{-\infty}^{\infty} \mathcal{A}(\boldsymbol{\kappa}_1, \boldsymbol{\kappa}_2) \\ &\quad \times \exp[i(\mathbf{k}_2 \cdot \mathbf{r}_2 - \mathbf{k}_1^* \cdot \mathbf{r}_1)] d^2\kappa_1 d^2\kappa_2, \end{aligned} \quad (9)$$

where the angular correlation matrix (ACM)

$$\begin{aligned} \mathcal{A}(\boldsymbol{\kappa}_1, \boldsymbol{\kappa}_2) &= \iiint \int_{-\infty}^{\infty} \mathcal{W}(\boldsymbol{\rho}_1, \boldsymbol{\rho}_2, 0) \\ &\quad \times \exp[i(\boldsymbol{\kappa}_1 \cdot \boldsymbol{\rho}_1 - \boldsymbol{\kappa}_2 \cdot \boldsymbol{\rho}_2)] d^2\rho_1 d^2\rho_2 \end{aligned} \quad (10)$$

describes the correlations between vectorial plane-wave components. In the far zone [17]

$$\begin{aligned} \mathcal{W}^\infty(r_1 \hat{\mathbf{s}}_1, r_2 \hat{\mathbf{s}}_2) &= (2\pi k)^2 \cos\theta_1 \cos\theta_2 \mathcal{A}(k\boldsymbol{\sigma}_1, k\boldsymbol{\sigma}_2) \\ &\quad \times \frac{\exp[ik(r_2 - r_1)]}{r_1 r_2} \end{aligned} \quad (11)$$

and the Poynting vector takes the form [17]

$$\begin{aligned} \mathbf{P}^\infty(r\hat{\mathbf{s}}) &= \frac{n\hat{\mathbf{s}}}{2} \sqrt{\frac{\epsilon_0}{\mu_0}} \text{tr } \mathcal{W}^\infty(r\hat{\mathbf{s}}, r\hat{\mathbf{s}}) \\ &= \hat{\mathbf{s}} \cos^2\theta \frac{2n\pi^2 k^2}{r^2} \sqrt{\frac{\epsilon_0}{\mu_0}} \text{tr } \mathcal{A}(k\boldsymbol{\sigma}, k\boldsymbol{\sigma}), \end{aligned} \quad (12)$$

where n is the refractive index of the material, and ϵ_0 and μ_0 are the vacuum permittivity and permeability, respectively. Furthermore, the radiant intensity is

$$\begin{aligned} J(r\hat{\mathbf{s}}) &= \lim_{r \rightarrow \infty} [r^2 \|\mathbf{P}^\infty(r\hat{\mathbf{s}})\|] \\ &= 2n\pi^2 k^2 \cos^2\theta \sqrt{\frac{\epsilon_0}{\mu_0}} \text{tr } \mathcal{A}(k\boldsymbol{\sigma}, k\boldsymbol{\sigma}). \end{aligned} \quad (13)$$

Owing to Eqs. (8) and (10), also ACM has a representation as a correlation matrix:

$$\mathcal{A}(\boldsymbol{\kappa}_1, \boldsymbol{\kappa}_2) = \langle \mathbf{A}^*(\boldsymbol{\kappa}_1) \mathbf{A}^T(\boldsymbol{\kappa}_2) \rangle, \quad (14)$$

where the components of $\mathbf{A}(\boldsymbol{\kappa})$ represent, component-wise, the angular spectra [1] of the electric-field realizations. It follows from Eq. (14) that $\mathcal{A}(\boldsymbol{\kappa}, \boldsymbol{\kappa})$ is Hermitian, satisfying

$$\mathcal{A}^\dagger(\boldsymbol{\kappa}_1, \boldsymbol{\kappa}_2) = \mathcal{A}(\boldsymbol{\kappa}_2, \boldsymbol{\kappa}_1), \quad (15)$$

where the dagger denotes the adjoint matrix. It is also non-negative definite in the sense that

$$\iiint \mathbf{a}^\dagger(\boldsymbol{\kappa}_1) \mathcal{A}(\boldsymbol{\kappa}_1, \boldsymbol{\kappa}_2) \mathbf{a}(\boldsymbol{\kappa}_2) d^2 \kappa_1 d^2 \kappa_2 \geq 0, \quad (16)$$

where $\mathbf{a}(\boldsymbol{\kappa})$ is an arbitrary, sufficiently well-behaved vector function of the same size as the electric-field vector.

The following argument is essential for the conclusions of this paper: the field in the far zone is well known to be a modulated outgoing spherical wave. Thus, in spherical polar coordinates, the angular-spectrum vector is two-dimensional, i.e., $\hat{\mathbf{s}} \cdot \mathbf{A}(k\boldsymbol{\sigma}) = 0$ for every $\hat{\mathbf{s}}$. Hence $\mathcal{A}(\boldsymbol{\kappa}_1, \boldsymbol{\kappa}_2)$ is expressible as a 2×2 matrix in these coordinates.

Since $\mathcal{A}(\boldsymbol{\kappa}_1, \boldsymbol{\kappa}_2)$ is a Hermitian, non-negative definite 2×2 matrix, it has two non-negative real-valued eigenfunctions. In view of Eqs. (15) and (16), we have at $\boldsymbol{\kappa}_1 = \boldsymbol{\kappa}_2 = \boldsymbol{\kappa}$ the decomposition

$$\mathcal{A}(\boldsymbol{\kappa}, \boldsymbol{\kappa}) = \sum_{j=1}^2 I_j(\boldsymbol{\kappa}) \mathbf{F}_j^*(\boldsymbol{\kappa}) \mathbf{F}_j^T(\boldsymbol{\kappa}), \quad (17)$$

where $I_j(\boldsymbol{\kappa})$ are the eigenvalues and $\mathbf{F}_j(\boldsymbol{\kappa})$ are the eigenvectors of $\mathcal{A}(\boldsymbol{\kappa}, \boldsymbol{\kappa})$. The eigenvectors may be assumed orthonormal, i.e.,

$$\mathbf{F}_p^\dagger(\boldsymbol{\kappa}) \mathbf{F}_q(\boldsymbol{\kappa}) = \delta_{pq}. \quad (18)$$

In other words, the matrix $\mathcal{A}(\boldsymbol{\kappa}, \boldsymbol{\kappa})$ can be diagonalized. Evaluation of the trace in Eq. (13) yields the explicit form for the radiant intensity:

$$J(r\hat{\mathbf{s}}) = J_0 \cos^2 \theta [I_1(k\boldsymbol{\sigma}) + I_2(k\boldsymbol{\sigma})], \quad (19)$$

where $J_0 = 2n\pi^2 k^2 \sqrt{\epsilon_0/\mu_0}$. Thus it is proportional to the sum of the eigenvalues of the ACM at $\boldsymbol{\kappa}_1 = \boldsymbol{\kappa}_2$.

The decomposition in Eq. (17) is, in fact, valid regardless of the chosen coordinate system; the eigenvalues remain invariant in all unitary transformations, including simple coordinate transformations between, e.g., Cartesian and spherical polar coordinate systems. As explicitly expressed in Eqs. (17), the polarization decomposition of ACM is generally direction-dependent: the eigenvalues and/or the eigenvectors depend on $\hat{\mathbf{s}}$.

The physical meaning of Eq. (17) is clear: In each direction in the far-zone, we may decompose the single-point ACM into two mutually uncorrelated, orthogonal polarization components. Moreover, owing to the factorized form $I_j(\boldsymbol{\kappa}) \mathbf{F}_j^*(\boldsymbol{\kappa}) \mathbf{F}_j^T(\boldsymbol{\kappa})$ of these components, they both represent fully polarized fields. This can be verified from the well-known formula for the (space-frequency domain) degree of polarization:

$$P(\mathbf{r}) = \left\{ 1 - \frac{4 \det \mathcal{W}(\mathbf{r}, \mathbf{r})}{[\text{tr } \mathcal{W}(\mathbf{r}, \mathbf{r})]^2} \right\}^{1/2}. \quad (20)$$

In the far zone we have, using Eq. (11),

$$P(r\hat{\mathbf{s}}) = \left\{ 1 - \frac{4 \det \mathcal{A}(k\boldsymbol{\sigma}, k\boldsymbol{\sigma})}{[\text{tr } \mathcal{A}(k\boldsymbol{\sigma}, k\boldsymbol{\sigma})]^2} \right\}^{1/2}. \quad (21)$$

With the aid of Eqs. (17) and (18), we then obtain

$$P(r\hat{\mathbf{s}}) = \left| \frac{I_1(k\boldsymbol{\sigma}) - I_2(k\boldsymbol{\sigma})}{I_1(k\boldsymbol{\sigma}) + I_2(k\boldsymbol{\sigma})} \right|. \quad (22)$$

Thus $P(r\hat{\mathbf{s}}) = 1$ for each individual polarization mode, i.e., if either $I_1(\boldsymbol{\kappa}) = 0$ or $I_2(\boldsymbol{\kappa}) = 0$. It is worth stressing that the polarization decomposition presented above is analogous with the well-known decomposition of a partially polarized plane wave into two polarization modes: in particular, Eq. (22) is analogous with Eq. (6.3-31) in Ref. [1]. In our case, however, the direction-dependent eigenvalues are those of a partially polarized and partially coherent field in the far zone.

To be able to include partial coherence (in addition to partial polarization) in the analysis, we now assume that also the two-point ACM can be expressed in the form

$$\mathcal{A}(\boldsymbol{\kappa}_1, \boldsymbol{\kappa}_2) = \mathcal{A}_1(\boldsymbol{\kappa}_1, \boldsymbol{\kappa}_2) + \mathcal{A}_2(\boldsymbol{\kappa}_1, \boldsymbol{\kappa}_2), \quad (23)$$

where $\mathcal{A}_j(\boldsymbol{\kappa}_1, \boldsymbol{\kappa}_2)$ have diagonal values $\mathcal{A}_j(\boldsymbol{\kappa}, \boldsymbol{\kappa}) = I_j(\boldsymbol{\kappa}) \mathbf{F}_j^*(\boldsymbol{\kappa}) \mathbf{F}_j^T(\boldsymbol{\kappa})$. In other words, $\mathcal{A}(\boldsymbol{\kappa}_1, \boldsymbol{\kappa}_2)$ is assumed to be expressible as a sum of two mutually uncorrelated, but fully coherent and polarized modes even if $\boldsymbol{\kappa}_1 \neq \boldsymbol{\kappa}_2$. We stress that, while Eq. (23) does not follow from Eq. (17), it typically holds. We do not dwell into a detailed discussion of this point here, but note that it is a nontrivial task to find counterexamples.

We proceed to investigate the angular correlation properties of the class of fields described by Eq. (23). Without loss of generality, we may employ spherical polar coordinates in the far field, in which case $\mathcal{A}_j(\boldsymbol{\kappa}_1, \boldsymbol{\kappa}_2)$ is a 2×2 matrix. Let us denote by $\mathcal{U}(\boldsymbol{\kappa})$ a unitary matrix whose columns are the eigenvectors $\mathbf{F}_j(\boldsymbol{\kappa})$ of $\mathcal{A}(\boldsymbol{\kappa}, \boldsymbol{\kappa})$ and by $\mathcal{D}(\boldsymbol{\kappa}, \boldsymbol{\kappa})$ a diagonal matrix with elements equal to the eigenvalues $I_j(\boldsymbol{\kappa})$ of $\mathcal{A}(\boldsymbol{\kappa}, \boldsymbol{\kappa})$. Then, equivalently with Eq. (17), we may write

$$\mathcal{A}(\boldsymbol{\kappa}, \boldsymbol{\kappa}) = \mathcal{U}^*(\boldsymbol{\kappa}) \mathcal{D}(\boldsymbol{\kappa}, \boldsymbol{\kappa}) \mathcal{U}^T(\boldsymbol{\kappa}) \quad (24)$$

and consequently

$$\mathcal{U}^T(\boldsymbol{\kappa}) \mathcal{A}(\boldsymbol{\kappa}, \boldsymbol{\kappa}) \mathcal{U}^*(\boldsymbol{\kappa}) = \mathcal{D}(\boldsymbol{\kappa}, \boldsymbol{\kappa}). \quad (25)$$

In view of Eq. (23) and the associated discussion, $\mathcal{A}_j(\boldsymbol{\kappa}_1, \boldsymbol{\kappa}_2)$ represents the angular correlation between two plane-wave components whose polarization states are described by deterministic vectors $\mathbf{F}_j(\boldsymbol{\kappa}_1)$ and $\mathbf{F}_j(\boldsymbol{\kappa}_2)$. Thus we may write, in analogy with Eq. (17),

$$\mathcal{A}(\boldsymbol{\kappa}_1, \boldsymbol{\kappa}_2) = \sum_{j=1}^2 G_j(\boldsymbol{\kappa}_1, \boldsymbol{\kappa}_2) \mathbf{F}_j^*(\boldsymbol{\kappa}_1) \mathbf{F}_j^T(\boldsymbol{\kappa}_2), \quad (26)$$

where $G_j(\boldsymbol{\kappa}_1, \boldsymbol{\kappa}_2)$ are scalar (angular correlation) functions. It is seen by direct calculation that $\mathcal{A}(\boldsymbol{\kappa}_1, \boldsymbol{\kappa}_2)$ has a representation similar to Eq. (25),

$$\mathcal{U}^T(\boldsymbol{\kappa}_1) \mathcal{A}(\boldsymbol{\kappa}_1, \boldsymbol{\kappa}_2) \mathcal{U}^*(\boldsymbol{\kappa}_2) = \mathcal{D}(\boldsymbol{\kappa}_1, \boldsymbol{\kappa}_2), \quad (27)$$

where $\mathcal{D}(\boldsymbol{\kappa}_1, \boldsymbol{\kappa}_2)$ is a diagonal matrix with elements $G_j(\boldsymbol{\kappa}_1, \boldsymbol{\kappa}_2)$. Thus $\mathbf{F}_j(\boldsymbol{\kappa})$ and $G_j(\boldsymbol{\kappa}_1, \boldsymbol{\kappa}_2)$ can be determined by singular value decomposition of $\mathcal{A}(\boldsymbol{\kappa}_1, \boldsymbol{\kappa}_2)$.

It can be shown, e.g., using Eq. (16) that the singular values $G_j(\boldsymbol{\kappa}_1, \boldsymbol{\kappa}_2)$ satisfy

$$|G_j(\boldsymbol{\kappa}_1, \boldsymbol{\kappa}_2)|^2 \leq I_j(\boldsymbol{\kappa}_1)I_j(\boldsymbol{\kappa}_2). \quad (28)$$

As a result, we may define the normalized angular correlation functions

$$g_j(\boldsymbol{\kappa}_1, \boldsymbol{\kappa}_2) = \frac{G_j(\boldsymbol{\kappa}_1, \boldsymbol{\kappa}_2)}{[I_j(\boldsymbol{\kappa}_1)I_j(\boldsymbol{\kappa}_2)]^{1/2}} \quad (29)$$

satisfying the inequalities $0 \leq |g_j(\boldsymbol{\kappa}_1, \boldsymbol{\kappa}_2)| \leq 1$. If the correlations in the far zone are of (generalized) Schell-model form, i.e., $g_j(\boldsymbol{\kappa}_1, \boldsymbol{\kappa}_2) = g_j(\Delta\boldsymbol{\kappa})$, it follows from Eqs. (26) and (29) that

$$\mathcal{A}(\boldsymbol{\kappa}_1, \boldsymbol{\kappa}_2) = \sum_{j=1}^2 g_j(\Delta\boldsymbol{\kappa}) \mathbf{f}_j^*(\boldsymbol{\kappa}_1) \mathbf{f}_j^T(\boldsymbol{\kappa}_2) \quad (30)$$

with

$$\mathbf{f}_j(\boldsymbol{\kappa}) = [I_j(\boldsymbol{\kappa})]^{1/2} \mathbf{F}_j(\boldsymbol{\kappa}). \quad (31)$$

This is the electromagnetic extension of Eq. (2).

5. Elementary electric-field modes

It follows from Eq. (23) and the linearity of Eq. (10) that the CSD has the decomposition

$$\mathcal{W}(\mathbf{r}_1, \mathbf{r}_2) = \mathcal{W}_1(\mathbf{r}_1, \mathbf{r}_2) + \mathcal{W}_2(\mathbf{r}_1, \mathbf{r}_2). \quad (32)$$

Let us define the inverse Fourier transforms $\mathbf{e}_j(\mathbf{r})$ and $p_j(\boldsymbol{\rho})$ of the functions $\mathbf{f}_j(\boldsymbol{\kappa})$ and $g_j(\Delta\boldsymbol{\kappa})$ in analogy with Eqs. (5) and (6). With a procedure similar to that used in derivation of Eq. (7), we can express the two terms in Eq. (32) in the form

$$\mathcal{W}_j(\mathbf{r}_1, \mathbf{r}_2) = \iint_{-\infty}^{\infty} p_j(\boldsymbol{\rho}') \mathbf{e}_j^*(\mathbf{r}_1 - \boldsymbol{\rho}') \mathbf{e}_j^T(\mathbf{r}_2 - \boldsymbol{\rho}') d^2 \rho' \quad (33)$$

in the half-space $z \geq 0$. In particular, Eq. (33) is valid at the source plane $z = 0$, where $\mathbf{e}_j(\mathbf{r}) = \mathbf{e}_j(\boldsymbol{\rho}, 0)$. This result is the electromagnetic extension of the scalar elementary-mode decomposition in Eq. (7).

Let us next examine some general properties of Eq. (33). Equations (18) and (31) together with

$$\mathbf{f}_j(\boldsymbol{\kappa}) = \iint_{-\infty}^{\infty} \mathbf{e}_j(\mathbf{r}) \exp(-i\boldsymbol{\kappa} \cdot \mathbf{r}) d^2 \rho \quad (34)$$

lead to

$$\iiint \iiint_{-\infty}^{\infty} \mathbf{e}_1^\dagger(\boldsymbol{\rho} - \boldsymbol{\rho}', 0) \mathbf{e}_2(\boldsymbol{\rho}, 0) \exp(-i\boldsymbol{\kappa} \cdot \boldsymbol{\rho}') d^2 \rho d^2 \rho' = 0. \quad (35)$$

Because of the exponential factor in the integral, $\mathbf{e}_1(\boldsymbol{\rho}, 0)$ and $\mathbf{e}_2(\boldsymbol{\rho}, 0)$ are generally not orthogonal in a pointwise sense. For many paraxial fields, though, the functions $\mathbf{f}_1(\boldsymbol{\kappa})$ and $\mathbf{f}_2(\boldsymbol{\kappa})$ are globally orthogonal, i.e., $\mathbf{f}_1^\dagger(\boldsymbol{\kappa}_1) \mathbf{f}_2(\boldsymbol{\kappa}_2) = 0$ for all $\boldsymbol{\kappa}_1$ and $\boldsymbol{\kappa}_2$. In this special case the pointwise orthogonality of $\mathbf{e}_1(\boldsymbol{\rho}, 0)$ and $\mathbf{e}_2(\boldsymbol{\rho}, 0)$ follows from Eqs. (18), (31), and (34). This property holds also for significant classes of non-paraxial fields, as will be demonstrated in Sections 6 and 8. However, it is not essential for practical implementation of the propagation algorithm developed in this paper.

Since the functions $\mathbf{e}_j(\mathbf{r})$ represent fully coherent fields, they obey the Helmholtz equation

$$\nabla^2 \mathbf{e}_j(\mathbf{r}) + k^2 \mathbf{e}_j(\mathbf{r}) = 0. \quad (36)$$

Furthermore, the CSD matrix obeys the divergence equation [4]

$$\nabla_1^T \mathcal{W}(\mathbf{r}_1, \mathbf{r}_2) = \mathbf{0}, \quad (37)$$

where the subscript 1 denotes differentiation with respect to \mathbf{r}_1 . Together with Eqs. (32) and (33), this implies that

$$\nabla \cdot \mathbf{e}_j(\mathbf{r}) = 0. \quad (38)$$

In view of Eqs. (36) and (38), the functions $\mathbf{f}_j(\mathbf{r})$ behave exactly as the electric field vector in the space-frequency domain. Hence the matrix-functions

$$\mathcal{W}_j^e(\mathbf{r}_1, \mathbf{r}_2) = \mathbf{e}_j^*(\mathbf{r}_1) \mathbf{e}_j^T(\mathbf{r}_2) \quad (39)$$

may be called the *elementary electric-field modes* of the field. Using these modes, we can write Eqs. (32) and (33) in a more compact form

$$\mathcal{W}(\mathbf{r}_1, \mathbf{r}_2) = \sum_{j=1}^2 \iint_{-\infty}^{\infty} p_j(\boldsymbol{\rho}') \mathcal{W}_j^e(\mathbf{r}_1 - \boldsymbol{\rho}', \mathbf{r}_2 - \boldsymbol{\rho}') d^2 \rho' \quad (40)$$

and express the spectral density of the field as

$$S(\mathbf{r}) = \sum_{j=1}^2 \iint_{-\infty}^{\infty} p_j(\boldsymbol{\rho}') S_j^e(\mathbf{r} - \boldsymbol{\rho}') d^2 \rho', \quad (41)$$

where $S_j^e(\mathbf{r}) = \text{tr } \mathcal{W}_j^e(\mathbf{r}, \mathbf{r})$ are the spectral densities of the two elementary electric-field modes.

In analogy with scalar theory [13], the field in Eq. (40) is understood to consist of a weighted continuum of identical, laterally shifted elementary modes. The main difference between the scalar and electromagnetic descriptions is that the electromagnetic field consists of two (uncorrelated) sets of elementary modes, whose polarization states in the far-zone are orthogonal and whose radiant-intensity distributions are in general different. Owing to the factorized form of $\mathcal{W}_j^e(\mathbf{r}_1, \mathbf{r}_2)$ in Eq. (39), each elementary mode is completely coherent [18] in the sense of the space-frequency analog of the degree of coherence for electromagnetic fields put forward in Ref. [19]:

$$\mu(\mathbf{r}_1, \mathbf{r}_2) = \{\text{tr } [\boldsymbol{\mu}(\mathbf{r}_1, \mathbf{r}_2) \boldsymbol{\mu}(\mathbf{r}_2, \mathbf{r}_1)]\}^{1/2}. \quad (42)$$

Here

$$\boldsymbol{\mu}(\mathbf{r}_1, \mathbf{r}_2) = \frac{\mathcal{W}(\mathbf{r}_1, \mathbf{r}_2)}{[S(\mathbf{r}_1)S(\mathbf{r}_2)]^{1/2}} \quad (43)$$

is the normalized CSD matrix. In general, all 3×3 matrix elements of $\mathcal{W}_j^e(\mathbf{r}_1, \mathbf{r}_2)$ are non-zero and spatially varying.

Analogously with Eqs. (42) and (43), we can define the degree of angular coherence

$$\alpha(\boldsymbol{\kappa}_1, \boldsymbol{\kappa}_2) = \{\text{tr}[\boldsymbol{\alpha}(\boldsymbol{\kappa}_1, \boldsymbol{\kappa}_2)\boldsymbol{\alpha}(\boldsymbol{\kappa}_2, \boldsymbol{\kappa}_1)]\}^{1/2} \quad (44)$$

where

$$\boldsymbol{\alpha}(\boldsymbol{\kappa}_1, \boldsymbol{\kappa}_2) = \frac{\mathcal{A}(\boldsymbol{\kappa}_1, \boldsymbol{\kappa}_2)}{[\text{tr} \mathcal{A}(\boldsymbol{\kappa}_1, \boldsymbol{\kappa}_1)\text{tr} \mathcal{A}(\boldsymbol{\kappa}_2, \boldsymbol{\kappa}_2)]^{1/2}} \quad (45)$$

is normalized angular correlation matrix.

To conclude this section we provide a convenient, fully general series representation for the electric-field modes. In the far zone, where the field is transverse to the local propagation direction and thus fluctuates locally in the plane defined by the spherical polar unit vectors $\hat{\boldsymbol{\theta}}$ and $\hat{\boldsymbol{\psi}}$, it is natural to express the basis vectors in the form

$$\mathbf{f}_j(\boldsymbol{\kappa}) = f_{j,\theta}(\boldsymbol{\kappa})\hat{\boldsymbol{\theta}} + f_{j,\psi}(\boldsymbol{\kappa})\hat{\boldsymbol{\psi}}. \quad (46)$$

Using spherical polar coordinates (θ, ψ) for the spatial frequencies and circular cylindrical coordinates (ρ, ϕ, z) for the position vector (see Fig. 1), we then have (after somewhat lengthy calculations outlined in Appendix A)

$$\begin{aligned} \mathbf{e}_j(\mathbf{r}) = & \frac{k}{2\pi} \sum_{m=-\infty}^{\infty} i^m \exp(im\phi) \int_0^{\pi/2} \exp(ikz \cos \theta) \\ & \times \left\{ \hat{\boldsymbol{\theta}} \left[-\frac{m}{\rho} f_{j,\psi,m}(\theta) - i \cos \theta f_{j,\theta,m}(\theta) \frac{d}{d\rho} \right] \right. \\ & + \hat{\boldsymbol{\psi}} \left[\frac{m}{\rho} \cos \theta f_{j,\theta,m}(\theta) - i f_{j,\psi,m}(\theta) \frac{d}{d\rho} \right] \\ & \left. - \hat{\mathbf{z}} k \sin^2 \theta f_{j,\theta,m}(\theta) \right\} J_m(k\rho \sin \theta) d\theta, \quad (47) \end{aligned}$$

where

$$f_{j,\xi,m}(\theta) = \frac{1}{2\pi} \int_0^{2\pi} f_{j,\xi}(\theta, \psi) \exp(-im\psi) d\psi \quad (48)$$

are the azimuthal Fourier coefficients of $f_{j,\xi}(\theta, \psi)$ and ξ stands for either θ or ψ . Note that the upper limit of the integral in Eq. (47) is set to $\pi/2$. Thus the elementary electric-field modes are taken to contain only propagating waves, i.e., information that can be gathered from far-zone measurements. As a result, the propagation method considered here is not suitable for modeling near-field phenomena (fields at distances of the order of one wavelength from the plane $z = 0$).

6. Rotationally symmetric fields

Let us assume that the CSD at $z = 0$ is rotationally symmetric about the z axis. Then also the ACM is rotationally symmetric and the polarization basis vectors $\mathbf{f}_1(\boldsymbol{\kappa})$ and $\mathbf{f}_2(\boldsymbol{\kappa})$ are rotationally invariant, i.e., their θ and ψ components $f_{j,\theta}(\theta, \psi)$ and $f_{j,\psi}(\theta, \psi)$ are independent on the azimuthal angle ψ . Hence only the zeroth-order Fourier coefficients $f_{j,\xi,0}(\theta)$ in Eq. (48) are non-zero and it follows from Eqs. (47) and (A14) that

$$\begin{aligned} \mathbf{e}_j(\mathbf{r}) = & \frac{k^2}{2\pi} \int_0^{\pi/2} \sin \theta \exp(ikz \cos \theta) \\ & \times \left\{ iJ_1(k\rho \sin \theta) [\cos \theta f_{j,\theta,0}(\theta)\hat{\boldsymbol{\rho}} + f_{j,\psi,0}(\theta)\hat{\boldsymbol{\phi}}] \right. \\ & \left. - \sin \theta J_0(k\rho \sin \theta) f_{j,\theta,0}(\theta)\hat{\mathbf{z}} \right\} d\theta. \quad (49) \end{aligned}$$

Thus, as expected, the elementary electric-field modes are also rotationally symmetric about the z axis. In particular, if the basis vectors are parallel to $\hat{\boldsymbol{\theta}}$ and $\hat{\boldsymbol{\psi}}$,

$$\begin{aligned} \mathbf{e}_1(\mathbf{r}) = & \frac{k^2}{2\pi} \int_0^{\pi/2} f_{j,\theta,0}(\theta) \sin \theta \\ & \times [i\hat{\boldsymbol{\rho}} J_1(k\rho \sin \theta) \cos \theta - \hat{\mathbf{z}} \sin \theta J_0(k\rho \sin \theta)] \\ & \times \exp(ikz \cos \theta) d\theta, \quad (50a) \end{aligned}$$

$$\begin{aligned} \mathbf{e}_2(\mathbf{r}) = & \hat{\boldsymbol{\phi}} \frac{ik^2}{2\pi} \int_0^{\pi/2} f_{j,\psi,0}(\theta) \sin \theta J_1(k\rho \sin \theta) \\ & \times \exp(ikz \cos \theta) d\theta. \quad (50b) \end{aligned}$$

The elementary modes $\mathbf{e}_1(\mathbf{r})$ and $\mathbf{e}_2(\mathbf{r})$ are now radially and azimuthally polarized fields, respectively. Hence they are pointwise orthogonal, regardless of whether the field is paraxial or not. Since these modes have no azimuthal phase variation, they possess no phase singularity (vortex) at $\rho = 0$. Thus, even if the axial field vanished $z = 0$ (as turns out to be often the case for some of the field components), such a zero does not propagate.

7. Quasi-homogeneous sources

Assume next that the variations of the spectral density $S(\boldsymbol{\rho}, 0)$ at the source plane are slow compared to the variations of the degree of coherence $\mu(\boldsymbol{\rho}_1, 0, \boldsymbol{\rho}_2, 0)$. Moreover, let the correlations at $z = 0$ be of the Schell-model form, i.e., depend only on $\Delta\boldsymbol{\rho} = \boldsymbol{\rho}_2 - \boldsymbol{\rho}_1$. Such a planar source is said to be quasi-homogeneous [1]. We may then approximate $S(\boldsymbol{\rho}_1, 0) \approx S(\boldsymbol{\rho}_2, 0) \approx S(\bar{\boldsymbol{\rho}}, 0)$, where $\bar{\boldsymbol{\rho}} = (\boldsymbol{\rho}_1 + \boldsymbol{\rho}_2)/2$, and write

$$\mathcal{W}(\boldsymbol{\rho}_1, \boldsymbol{\rho}_2, 0) \approx S(\bar{\boldsymbol{\rho}}, 0)\mu(\Delta\boldsymbol{\rho}, 0). \quad (51)$$

Inserting Eq. (51) into Eq. (10) and defining $\bar{\boldsymbol{\kappa}} = (\boldsymbol{\kappa}_1 + \boldsymbol{\kappa}_2)/2$ yields

$$\mathcal{A}(\boldsymbol{\kappa}_1, \boldsymbol{\kappa}_2) = \tilde{S}(\Delta\boldsymbol{\kappa})\tilde{\mu}(\bar{\boldsymbol{\kappa}}), \quad (52)$$

where

$$\tilde{S}(\Delta\boldsymbol{\kappa}) = \iint_{-\infty}^{\infty} S(\bar{\boldsymbol{\rho}}, 0) \exp(-i\Delta\boldsymbol{\kappa} \cdot \bar{\boldsymbol{\rho}}) d^2\bar{\boldsymbol{\rho}}, \quad (53)$$

and

$$\tilde{\boldsymbol{\mu}}(\bar{\boldsymbol{\kappa}}) = \iint_{-\infty}^{\infty} \boldsymbol{\mu}(\Delta\boldsymbol{\rho}, 0) \exp(-i\bar{\boldsymbol{\kappa}} \cdot \Delta\boldsymbol{\rho}) d^2\Delta\boldsymbol{\rho}. \quad (54)$$

Since

$$\begin{aligned} \text{tr } \mathcal{A}(\boldsymbol{\kappa}, \boldsymbol{\kappa}) &= \tilde{S}(\mathbf{0}) \text{tr } \tilde{\boldsymbol{\mu}}(\boldsymbol{\kappa}) \\ &= \tilde{S}(\mathbf{0}) \iint_{-\infty}^{\infty} \text{tr } \boldsymbol{\mu}(\Delta\boldsymbol{\rho}, 0) \exp(-i\boldsymbol{\kappa} \cdot \Delta\boldsymbol{\rho}) d^2\Delta\boldsymbol{\rho}, \end{aligned} \quad (55)$$

it follows from Eq. (13) that the radiant intensity produced by a quasihomogeneous electromagnetic source depends only on the correlation properties of the source field, in complete analogy with the scalar case [1].

Inserting from Eq. (51) into Eq. (45) and recalling that $\tilde{\boldsymbol{\mu}}$ is a wide function compared to \tilde{S} , we have

$$\boldsymbol{\alpha}(\boldsymbol{\kappa}_1, \boldsymbol{\kappa}_2) = \frac{\tilde{S}(\Delta\boldsymbol{\kappa})}{\tilde{S}(\mathbf{0})} \frac{\tilde{\boldsymbol{\mu}}(\bar{\boldsymbol{\kappa}})}{\tilde{\boldsymbol{\mu}}(\mathbf{0})}. \quad (56)$$

Using Eq. (44) and noting that \tilde{S} is real because S is non-negative, we obtain

$$\alpha(\boldsymbol{\kappa}_1, \boldsymbol{\kappa}_2) = \frac{\tilde{S}(\Delta\boldsymbol{\kappa})}{\tilde{S}(\mathbf{0})} \frac{\left\{ \text{tr } [\tilde{\boldsymbol{\mu}}(\bar{\boldsymbol{\kappa}})]^2 \right\}^{1/2}}{\text{tr } \tilde{\boldsymbol{\mu}}(\bar{\boldsymbol{\kappa}})}. \quad (57)$$

This expression can be cast into a more transparent form using the far-zone degree of polarization defined in Eq. (21), which can be written equivalently in the form

$$P(\boldsymbol{\kappa}) = \left\{ \frac{2 \text{tr } [\tilde{\boldsymbol{\mu}}(\boldsymbol{\kappa})]^2}{[\text{tr } \tilde{\boldsymbol{\mu}}(\boldsymbol{\kappa})]^2} - 1 \right\}^{1/2}. \quad (58)$$

We then have, from Eq. (57),

$$\alpha(\boldsymbol{\kappa}_1, \boldsymbol{\kappa}_2) = \frac{\tilde{S}(\Delta\boldsymbol{\kappa})}{\tilde{S}(\mathbf{0})} \left[\frac{D^2(\bar{\boldsymbol{\kappa}}) + 1}{2} \right]^{1/2}. \quad (59)$$

The first fraction in this expression is equal to the scalar degree of angular coherence. The second fraction, however, is a polarization-dependent modulating term that depends on the source-plane correlations.

The assumption that the source is quasihomogeneous simplifies decisively the elementary-mode decomposition of the field in the scalar case [13], and the same is true in the electromagnetic case. It follows from Eqs. (17), (31), and (34) that

$$\begin{aligned} &\sum_{j=1}^2 \iint_{-\infty}^{\infty} \mathbf{e}_j^*(\boldsymbol{\rho}_1 - \boldsymbol{\rho}', 0) \mathbf{e}_j^T(\boldsymbol{\rho}_2 - \boldsymbol{\rho}', 0) d^2\boldsymbol{\rho}' \\ &= \frac{1}{(2\pi)^2} \iint_{-\infty}^{\infty} \mathcal{A}(\boldsymbol{\kappa}, \boldsymbol{\kappa}) \exp(i\boldsymbol{\kappa} \cdot \Delta\boldsymbol{\rho}) d^2\boldsymbol{\kappa} \\ &= \tilde{S}(\mathbf{0}) \boldsymbol{\mu}(\Delta\boldsymbol{\rho}, 0), \end{aligned} \quad (60)$$

where, in the last step, we have used Eq. (52). Comparing Eqs. (51) and (60) yields

$$\begin{aligned} \mathcal{W}(\boldsymbol{\rho}_1, \boldsymbol{\rho}_2, 0) &\approx \frac{S(\bar{\boldsymbol{\rho}}, 0)}{\tilde{S}(\mathbf{0})} \\ &\times \sum_{j=1}^2 \iint_{-\infty}^{\infty} \mathbf{e}_j^*(\boldsymbol{\rho}_1 - \boldsymbol{\rho}', 0) \mathbf{e}_j^T(\boldsymbol{\rho}_2 - \boldsymbol{\rho}', 0) d^2\boldsymbol{\rho}'. \end{aligned} \quad (61)$$

Thus the weight function no longer appears inside the integral and, irrespective of the spatial distribution of the spectral density at the source plane, the field characteristics can be determined the propagating a convolution integral involving the elementary modes only.

8. Sources with cosine-power radiant intensity

Let us consider the rotationally symmetric case with radially and azimuthally polarized basis vectors $\mathbf{F}_1(\theta, \psi) = \hat{\boldsymbol{\theta}}$, $\mathbf{F}_2(\theta, \psi) = \hat{\boldsymbol{\psi}}$, and corresponding eigenvalues $I_1(\theta, \psi) = A_1^2 \cos^{a-2} \theta$, $I_2(\theta, \psi) = A_2^2 \cos^{b-2} \theta$, where A_1 and A_2 are arbitrary (real) functions of frequency. Then, in view of Eq. (19), the radiant intensity is a superposition of two $\cos^n \theta$ type contributions, one radially and the other azimuthally polarized:

$$J(\theta, \psi) = J_0 [A_1^2 \cos^a \theta + A_2^2 \cos^b \theta]. \quad (62)$$

The elementary electric-field modes in the far zone are, according to Eq. (31),

$$\mathbf{f}_1(\theta, \psi) = \hat{\boldsymbol{\theta}} A_1 \cos^{a/2-1} \theta, \quad (63a)$$

$$\mathbf{f}_2(\theta, \psi) = \hat{\boldsymbol{\psi}} A_2 \cos^{b/2-1} \theta. \quad (63b)$$

Using Eqs. (46) and (48) we see that the non-vanishing Fourier coefficients are $f_{1,\theta,0} = A_1 \cos^{a/2-1} \theta$ and $f_{2,\psi,0} = A_2 \cos^{b/2-1} \theta$. Inserting these into Eqs. (50) and applying (B4b) derived in Appendix B, we obtain the source-plane elementary field modes in the form

$$\begin{aligned} \mathbf{e}_1(\boldsymbol{\rho}, 0) &= A_1 \frac{ik^2}{8\sqrt{\pi}} \left[\hat{\boldsymbol{\rho}} \frac{k\rho}{2} \Gamma\left(\frac{1}{2} + \frac{a}{4}\right) \right. \\ &\times {}_1\tilde{F}_2\left(\frac{3}{2}; 2, 2 + \frac{a}{4}; -\frac{k^2\rho^2}{4}\right) \\ &\left. - \hat{\mathbf{z}} \Gamma\left(\frac{a}{4}\right) {}_1\tilde{F}_2\left(\frac{3}{2}; 1, \frac{3}{2} + \frac{a}{4}; -\frac{k^2\rho^2}{4}\right) \right], \end{aligned} \quad (64a)$$

$$\begin{aligned} \mathbf{e}_2(\boldsymbol{\rho}, 0) &= \hat{\phi} A_2 \frac{ik^3\rho}{16\sqrt{\pi}} \Gamma\left(\frac{b}{4}\right) \\ &\times {}_1\tilde{F}_2\left(\frac{3}{2}; 2, \frac{3}{2} + \frac{b}{4}; -\frac{k^2\rho^2}{4}\right), \end{aligned} \quad (64b)$$

where Γ is the Gamma function and ${}_1\tilde{F}_2$ is the regularized hypergeometric function (see Appendix B).

Figures 2–4 illustrate the radial dependence of the elementary-field components and the function

$$w(\boldsymbol{\rho}, 0) = [\|\mathbf{e}_1(\boldsymbol{\rho}, 0)\|^2 + \|\mathbf{e}_2(\boldsymbol{\rho}, 0)\|^2]^{1/2} \quad (65)$$

for different values of $a = b = n$, with $A_1 = A_2 = -ik^{-2}$.

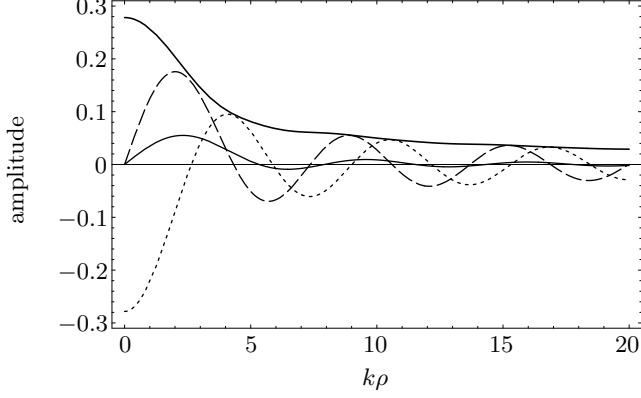


Fig. 2. Relative amplitudes of the radial (solid line), azimuthal (dashed line), and longitudinal (dotted line) components of the elementary fields as a function of the normalized radial coordinate $k\rho$, as well as the function $w(k\rho)$ (thick solid line) for $n = 1$, which corresponds to a Lambertian source.

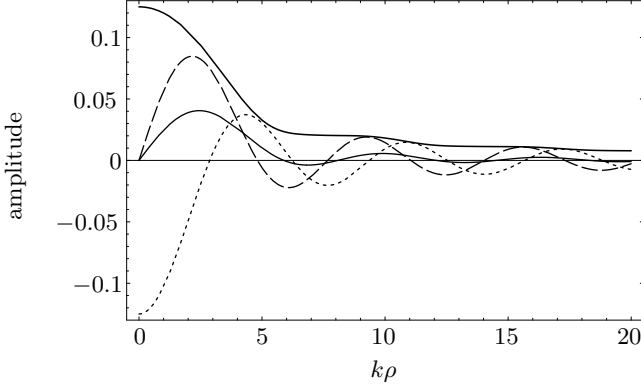


Fig. 3. Same as Fig. 2, but with $n = 2$, which corresponds to an incoherent source in scalar theory.

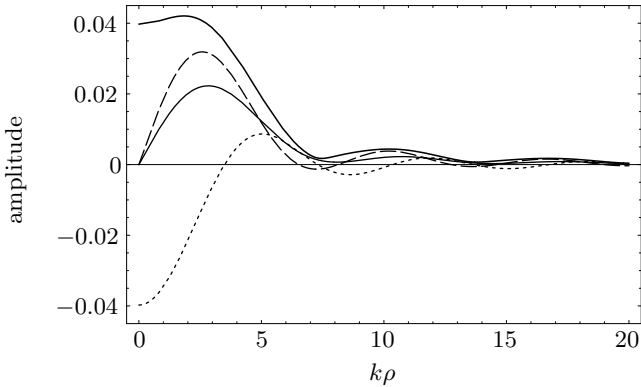


Fig. 4. Same as Fig. 2, but with $n = 5$. Thus the source has a somewhat directional radiation pattern.

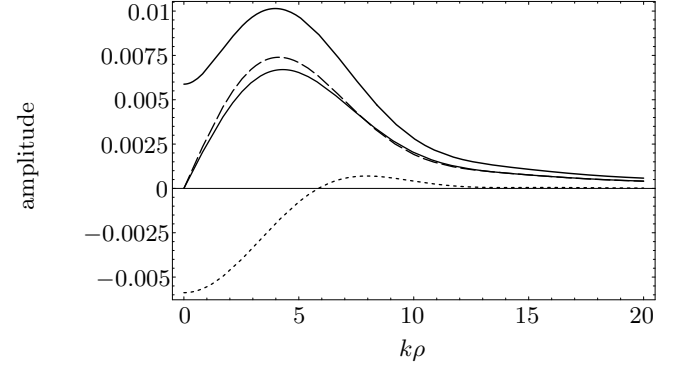


Fig. 5. Same as Fig. 4, but with $n = 20$. The radiation pattern is increasingly directional and could be produced approximately by a LED with an integrated collimating lens.

9. Illustration: LED model

Let us consider a simple model for a rotationally symmetric surface-emitting LED illustrated in Fig. 6a, where the primary light-emitting region is planar (such as a quantum well) and buried inside a semiconductor material of refractive index n_s . Each primary source point is assumed to radiate (independently) a spherical wave. If we denote the propagation angle inside the semiconductor material by θ' , the radiant intensity may be expressed as a sum of radially and azimuthally polarized contributions $J_j^{(i)}(\theta')$, $j = 1, 2$:

$$J_j^{(i)}(\theta') = J_{0,j}^{(i)} \cos^2 \theta' I_j^{(i)}(\theta') = J_{0,j}^{(i)} \cos^2 \theta' |A_j^{(i)}(\theta')|^2, \quad (66)$$

where $A_j^{(i)}(\theta')$ is the complex amplitude of the plane wave in direction θ' . If the distance between the pn plane and the semiconductor-air interface is large compared to λ , the local plane wave approximation is valid at the semiconductor-air interface. Thus the output radiant intensity takes the form

$$J_j(\theta) = J_{0,j} \cos^2 \theta I_j(\theta) = J_{0,j} \cos^2 \theta |A_j(\theta)|^2. \quad (67)$$

Here $J_{0,j} = J_{0,j}^{(i)}/n_s$, the angles θ and θ' are related by Snell's law $\sin \theta = n_s \sin \theta'$, and $A_j(\theta) = t_j(\theta, \theta') A_j(\theta')$, where $t_j(\theta, \theta')$ are given by Fresnel's equations

$$t_1(\theta, \theta') = \frac{2n_s \cos \theta}{\cos \theta' + n_s \cos \theta}, \quad (68)$$

$$t_2(\theta, \theta') = \frac{2 \cos \theta}{n_s \cos \theta' + \cos \theta} \quad (69)$$

for radial (TM) and azimuthal (TE) polarizations.

Because of the large refractive index n_s of a semiconductor, only a narrow cone of plane waves with incident

angles θ' in the range $0 \leq \theta' < \arcsin(1/n_s)$. We may thus assume that the radial and azimuthal contributions to the radiant intensity of the primary source are equal, i.e., $I_1^{(i)} = I_2^{(i)}$, and hence we may denote $J_0^{(i)} = 2J_{0,j}^{(i)}$ and $J_0 = 2J_{0,j}$. Then the degree of polarization given by Eq. (22) is

$$P(\theta) = \frac{|t_1(\theta, \theta')|^2 - |t_2(\theta, \theta')|^2}{|t_1(\theta, \theta')|^2 + |t_2(\theta, \theta')|^2} \quad (70)$$

and the radiant intensity transforms at the interface according to

$$\frac{J(\theta)}{J^{(i)}(\theta)} = \frac{1}{2n_s} \frac{\cos^2 \theta}{\cos^2 \theta'} \left[|t_1(\theta, \theta')|^2 + |t_2(\theta, \theta')|^2 \right]. \quad (71)$$

If we assume that the radiation pattern produced by the primary source is Lambertian, with

$$J_j^{(i)}(\theta') = \frac{1}{2} J_0^{(i)} \cos \theta', \quad (72)$$

the radial and azimuthal contributions to the radiant intensity of the secondary source become

$$J_j(\theta) = \frac{1}{2} J_0 \frac{\cos^2 \theta}{\cos \theta'} |t_j(\theta, \theta')|^2. \quad (73)$$

These contributions $J_1(\theta)$ and $J_2(\theta)$ are shown by the dotted and dashed lines, respectively, in Fig. 6b, where we have taken $n_s = 3.5$. The curves fit well the $\cos^n \theta$: we obtain $n \approx 3.4 = b$ for the azimuthally polarized contribution, $n \approx 2.4 = a$ for the radially polarized contribution, and $n \approx 2.9$ for an equally weighted sum of the two contributions. Thus the elementary electric-field modes given by Eq. (64) provide good approximations of the modes of the structure in Fig. 6a.

The degree of polarization, also plotted in Fig. 6b, increases from a zero on-axis value (unpolarized radiation in the paraxial domain) to $P(\theta) \approx 0.85$ when $\theta \rightarrow \pi/2$, indicating partially polarized radiation in the non-paraxial domain.

10. Final remarks

The electromagnetic elementary-mode decomposition presented in this paper should prove useful in optical system modeling by field tracing methods. To this end, it is necessary to determine elementary field modes and the weight functions of the source. The example presented above illustrates the possibility of doing this if there is sufficient a priori information about the structure of the source. If, however, the source properties are not known, it is necessary to determine the modal decomposition experimentally. As in the scalar case [13], this can in principle be accomplished by far-field measurements. In general, the polarization basis vectors \mathbf{f}_j and the eigenvalues I_j can be determined from the polarization matrix $\mathcal{A}(\boldsymbol{\kappa}, \boldsymbol{\kappa})$. This matrix can be determined by measuring, e.g., the angular dependence of the Stokes parameters of

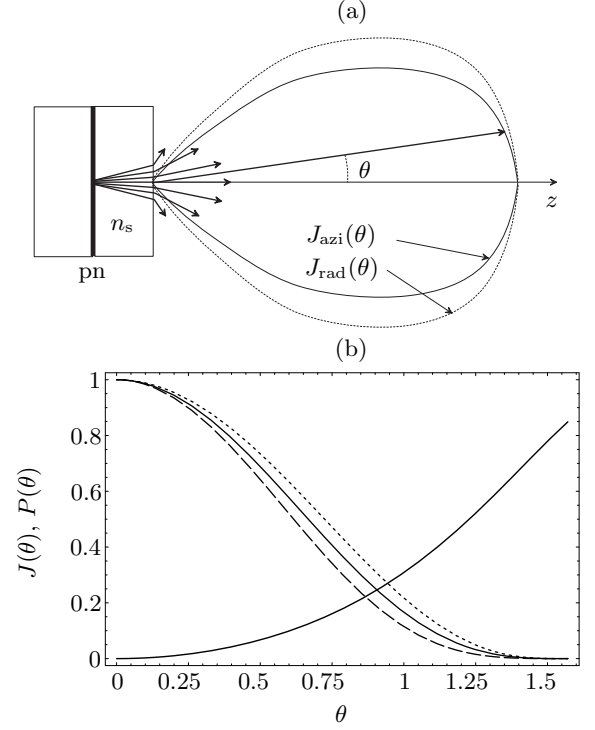


Fig. 6. (a) A generic geometry of a broad-area surface-emitting LED: pn is the active emitting area and n is the refractive index of the semiconductor material. The solid and dashed curves illustrate the azimuthally and radially polarized contributions to the radiant intensity distribution $J(\theta)$. (b) Geometrical-optics predictions of the azimuthally (dashed curve) and radially (dotted curve) polarized contributions to the radiant intensity, their average (solid curve), and the degree of polarization $P(\theta)$ in the far zone (thick solid curve).

the field in the far zone. Thus only single-point measurements across the radiation pattern are needed. Determination of the weight functions requires, in general, two-point correlation measurements in the far zone, but this is avoided if the field is known to be quasihomogeneous.

Acknowledgments

This work was supported by the Academy of Finland (118951, 129155, and 209806).

Appendix A: Derivation of Eq. (47)

In this Appendix we present some details of the derivation of Eq. (47), which is the general representation of the elementary electric-field modes. Denoting the circular cylindrical coordinates by (ρ, ϕ, z) in the position-vector space and by (κ, ψ, z) in the wave vector space, and the spherical polar coordinates by (k, θ, ψ) in the wave vector space, we have the following relations between the unit vectors of these systems and the Cartesian coordinates

(see Fig. 1):

$$\begin{bmatrix} \hat{\rho} \\ \hat{\phi} \end{bmatrix} = \mathbf{R}(\phi) \begin{bmatrix} \hat{\mathbf{x}} \\ \hat{\mathbf{y}} \end{bmatrix}, \quad (\text{A1})$$

$$\begin{bmatrix} \hat{\kappa} \\ \hat{\psi} \end{bmatrix} = \mathbf{R}(\psi) \begin{bmatrix} \hat{\mathbf{x}} \\ \hat{\mathbf{y}} \end{bmatrix}, \quad (\text{A2})$$

$$\begin{bmatrix} \hat{\mathbf{k}} \\ \hat{\theta} \end{bmatrix} = \mathbf{R}(\theta) \begin{bmatrix} \hat{\mathbf{z}} \\ \hat{\kappa} \end{bmatrix}, \quad (\text{A3})$$

where

$$\mathbf{R}(\xi) = \begin{bmatrix} \cos \xi & \sin \xi \\ -\sin \xi & \cos \xi \end{bmatrix} \quad (\text{A4})$$

is the rotation matrix and ξ may stand for ϕ , ψ , or θ . Using Eq. (A3) and recognizing that $k_z = k \cos \theta$ and $\kappa = k \sin \theta$, we can write Eq. (46) in circular cylindrical coordinates:

$$\mathbf{f}_j(\boldsymbol{\kappa}) = \cos \theta f_{j,\theta}(\boldsymbol{\kappa}) \hat{\kappa} + f_{j,\psi}(\boldsymbol{\kappa}) \hat{\psi} - \sin \theta f_{j,\theta}(\boldsymbol{\kappa}) \hat{\mathbf{z}}. \quad (\text{A5})$$

Using Eqs. (A1) and (A2) one can establish the relation

$$\begin{bmatrix} \hat{\kappa} \\ \hat{\psi} \end{bmatrix} = \frac{1}{2} \begin{bmatrix} 1 & 1 \\ -i & i \end{bmatrix} \begin{bmatrix} e^{i\beta} (\hat{\rho} + i\hat{\psi}) \\ e^{-i\beta} (\hat{\rho} - i\hat{\psi}) \end{bmatrix}, \quad (\text{A6})$$

where $\beta = \phi - \psi$, and express $\mathbf{f}_j(\boldsymbol{\kappa})$ in the form

$$\begin{aligned} \mathbf{f}_j(\theta, \psi) &= \frac{1}{2} [\cos \theta f_{j,\theta}(\theta, \psi) - i f_{j,\psi}(\theta, \psi)] e^{i\beta} (\hat{\rho} + i\hat{\psi}) \\ &+ \frac{1}{2} [\cos \theta f_{j,\theta}(\theta, \psi) + i f_{j,\psi}(\theta, \psi)] e^{-i\beta} (\hat{\rho} - i\hat{\psi}) \\ &- \sin \theta f_{j,\theta}(\theta, \psi) \hat{\mathbf{z}}. \end{aligned} \quad (\text{A7})$$

Recognizing further that $\mathbf{k} \cdot \mathbf{r} = \boldsymbol{\kappa} \cdot \boldsymbol{\rho} + k_z z$ and that $\boldsymbol{\kappa} \cdot \boldsymbol{\rho} = k\rho \sin \theta \cos \beta$, we can expand the plane-wave term in Eq. (6) in a series form

$$\exp(i\mathbf{k} \cdot \mathbf{r}) = \exp(ikz \cos \theta) \sum_{m=-\infty}^{\infty} i^m J_m(k\rho \sin \theta) e^{-im\beta}, \quad (\text{A8})$$

where J_m denotes the Bessel function of the first kind and order m . Combining Eqs. (??) and (A7) we then have

$$\begin{aligned} \mathbf{e}_j(\mathbf{r}) &= \frac{k}{2\pi} \sum_{m=-\infty}^{\infty} i^m \int_0^{\pi/2} \mathbf{g}_{j,m}(\mathbf{r}) \exp(ikz \cos \theta) \\ &\times J_m(k\rho \sin \theta) k \sin \theta d\theta, \end{aligned} \quad (\text{A9})$$

where

$$\mathbf{g}_{j,m}(\mathbf{r}) = \frac{1}{2\pi} \int_0^{2\pi} \mathbf{f}_j(\theta, \psi) e^{-im\beta} d\psi. \quad (\text{A10})$$

Performing the integration with respect to ψ with the aid of the definition of the azimuthal Fourier coefficients in Eq. (48), we obtain

$$\begin{aligned} \mathbf{g}_{j,m}(\mathbf{r}) &= \frac{1}{2} (\hat{\rho} + i\hat{\phi}) [\cos \theta f_{j,\theta,m+1}(\theta) - i f_{j,\psi,m+1}(\theta)] \\ &\times e^{i(m+1)\phi} J_m(k\rho \sin \theta) k \sin \theta \\ &+ \frac{1}{2} (\hat{\rho} - i\hat{\phi}) [\cos \theta f_{j,\theta,m-1}(\theta) + i f_{j,\psi,m-1}(\theta)] \\ &\times e^{i(m-1)\phi} J_m(k\rho \sin \theta) k \sin \theta \\ &- \hat{\mathbf{z}} e^{im\phi} J_m(k\rho \sin \theta) k \sin^2 \theta. \end{aligned} \quad (\text{A11})$$

Collecting terms in the summation of Eq. (A9) by replacements

$$e^{i(m\pm 1)\phi} J_m(k\rho \sin \theta) \rightarrow i^{\mp 1} e^{im\phi} J_{m\mp 1}(k\rho \sin \theta) \quad (\text{A12})$$

and employing the Bessel-function identities [20]

$$J_{m-1}(x) + J_{m+1}(x) = \frac{2m}{x} J_m(x) \quad (\text{A13})$$

and

$$J_{m-1}(x) - J_{m+1}(x) = 2 \frac{d}{dx} J_m(x) \quad (\text{A14})$$

we finally arrive at Eq. (47).

Appendix B: Derivation of an integral formula

Let us first recall the series-representation of Bessel functions [20]:

$$J_m(\gamma) = \sum_{j=0}^{\infty} \frac{(-1)^j}{j!(m+j)!} \left(\frac{\gamma}{2}\right)^{m+2j}. \quad (\text{B1})$$

On the other hand, we have the relation [21]

$$\int_0^{\pi/2} \sin^p \theta \cos^q \theta d\theta = \frac{1}{2} B\left(\frac{p+1}{2}, \frac{q+1}{2}\right), \quad (\text{B2})$$

where $\Re(p) > -1$, $\Re(q) > -1$,

$$B(\gamma, \xi) = \frac{\Gamma(\gamma)\Gamma(\xi)}{\Gamma(\gamma + \xi)} \quad (\text{B3})$$

is the beta function, and $\Gamma(\gamma)$ is the Gamma function [20]. Combining Eqs. (B1) and (B2), and interchanging the order of summation and integration yields

$$\begin{aligned} &\int_0^{\pi/2} \sin^p \theta \cos^q \theta J_m(k\rho \sin \theta) d\theta \\ &= \frac{(k\rho)^m}{2^{m+1}} \Gamma\left(\frac{q+1}{2}\right) \\ &\times \sum_{j=0}^{\infty} \frac{\Gamma[j + \frac{1}{2}(p+m+1)]}{j!\Gamma(m+j+1)\Gamma[j+1+\frac{1}{2}(p+m+q)]} \\ &\times \left(\frac{-k^2 \rho^2}{4}\right)^j, \end{aligned} \quad (\text{B4a})$$

where we have employed the identity $s! = \Gamma(s + 1)$ for integer s . Equation (B4a) can also be expressed in the form

$$\begin{aligned} & \int_0^{\pi/2} \sin^p \theta \cos^q \theta J_m(k\rho \sin \theta) d\theta \\ &= \frac{(k\rho)^m}{2^{m+1}} \Gamma\left(\frac{q+1}{2}\right) \Gamma\left(\frac{p+m+1}{2}\right) \\ & \times {}_1\tilde{F}_2\left(\frac{p+m+1}{2}; m+1, 1 + \frac{p+q+m}{2}; -\frac{k^2\rho^2}{4}\right), \end{aligned} \quad (\text{B4b})$$

where ${}_p\tilde{F}_q(a_1, a_2, \dots, a_p; b_1, b_2, \dots, b_q; \gamma)$ denotes the regularized hypergeometric function, defined by

$$\begin{aligned} & {}_p\tilde{F}_q(a_1, a_2, \dots, a_p; b_1, b_2, \dots, b_q; \gamma) \\ &= \frac{{}_pF_q(a_1, a_2, \dots, a_p; b_1, b_2, \dots, b_q; \gamma)}{\Gamma(b_1)\Gamma(b_2)\dots\Gamma(b_q)}, \end{aligned} \quad (\text{B5})$$

${}_pF_q(a_1, a_2, \dots, a_p; b_1, b_2, \dots, b_q; \gamma)$ is the generalized hypergeometric function [22]

$$\begin{aligned} & {}_pF_q(a_1, a_2, \dots, a_p; b_1, b_2, \dots, b_q; \gamma) \\ &= \sum_{j=0}^{\infty} \frac{(a_1)_j (a_2)_j \dots (a_p)_j \gamma^j}{j! (b_1)_j (b_2)_j \dots (b_q)_j} \end{aligned} \quad (\text{B6})$$

and

$$(c)_j = \frac{\Gamma(j+c)}{\Gamma(c)}. \quad (\text{B7})$$

References

1. L. Mandel and E. Wolf, *Optical Coherence and Quantum Optics* (Cambridge University Press, Cambridge, UK, 1995).
2. E. Wolf, “New theory of partial coherence in the space–frequency domain. Part I: Spectra and cross spectra of steady-state sources,” *J. Opt. Soc. Am.* **72**, 343–351 (1982).
3. F. Gori, M. Santarsiero, R. Simon, G. Piquero, R. Borghi, and G. Guattari, “Coherent-mode decomposition of partially coherent, partially polarized sources,” *J. Opt. Soc. Am. A* **20**, 78–84 (2003).
4. J. Tervo, T. Setälä, and A. T. Friberg, “Theory of partially coherent electromagnetic fields in the space–frequency domain,” *J. Opt. Soc. Am. A* **21**, 2205–2215 (2004).
5. F. Gori, “Collett-Wolf sources and multimode lasers,” *Opt. Commun.* **34**, 301–305 (1980).
6. F. Gori, “Mode propagation of the light field generated by Collett-Wolf Schell-model sources,” *Opt. Commun.* **46**, 149–154 (1983).
7. A. Starikov and E. Wolf, “Coherent-mode representation of Gaussian Schell-model sources and of their radiation fields,” *J. Opt. Soc. Am. A* **72**, 923–928 (1982).
8. A. Starikov, “Effective number of degrees of freedom of partially coherent sources,” *J. Opt. Soc. Am.* **73**, 1538–1544 (1983).
9. J. Huttunen, A. T. Friberg, and J. Turunen, “Diffraction of partially coherent electromagnetic fields by microstructured media,” *Phys. Rev. E* **52**, 3081–3092 (1995).
10. P. Vahimaa and J. Turunen, “Bragg diffraction of spatially partially coherent fields,” *J. Opt. Soc. Am. A* **14**, 54–59 (1997).
11. F. Gori and C. Palma, “Partially coherent sources which give rise to highly directional laser beams,” *Opt. Commun.* **27**, 185–188 (1978).
12. F. Gori, “Directionality and partial coherence,” *Opt. Acta* **27**, 1025–1034 (1980).
13. P. Vahimaa and J. Turunen, “Finite-elementary-source model for partially coherent radiation,” *Opt. Express* **14**, 1376–1381 (2006).
14. F. Gori and M. Santarsiero, “Devising genuine correlation functions,” *Opt. Lett.* **32**, 531–533 (2007).
15. J. Turunen and P. Vahimaa, “Independent-elementary-field model for three-dimensional spatially partially coherent sources,” *Opt. Express* **16**, 6433–6442 (2008).
16. M. A. Alonso and E. Wolf, “The cross-spectral density matrix of a planar, electromagnetic stochastic source as a correlation matrix,” *Opt. Commun.* **281**, 2393–2396 (2008).
17. J. Tervo and J. Turunen, “Angular spectrum representation of partially coherent electromagnetic fields,” *Opt. Commun.* **209**, 7–16 (2002).
18. T. Setälä, J. Tervo, and A. T. Friberg, “Complete electromagnetic coherence in space–frequency domain,” *Opt. Lett.* **29**, 328–330 (2004).
19. J. Tervo, T. Setälä, and A. T. Friberg, “Degree of coherence for electromagnetic fields,” *Opt. Express* **11**, 1137–1143 (2003).
20. G. B. Arfken and H. J. Weber, *Mathematical Methods for Physicists*, 5th ed. (Academic Press, San Diego, CA, 2001).
21. I. S. Gradshteyn and I. M. Ryzhik, *Table of Integrals, Series, and Products*, A. Jeffrey, D. Zwillinger, eds., seventh edition. (Academic Press, Orlando, 2007).
22. W. N. Bailey, *Generalized Hypergeometric Series*, Vol. 32 of Cambridge Tracts in Mathematics and Mathematical Physics, G. H. Hardy and E. Cunningham, eds. (Cambridge University Press, Cambridge, UK, 1935).